

Probing $e\mu$ flavor-violating ALP at Belle II

Motoi Endo^(a,b), Syuhei Iguro^(c), and Teppei Kitahara^(d,e,f)

^(a)*KEK Theory Center, IPNS, KEK, Tsukuba 305-0801, Japan*

^(b)*The Graduate University of Advanced Studies (Sokendai), Tsukuba 305-0801, Japan*

^(c)*Department of Physics, Nagoya University, Nagoya 464-8602, Japan*

^(d)*Physics Department, Technion–Israel Institute of Technology, Haifa 3200003, Israel*

^(e)*Institute for Advanced Research, Nagoya University, Nagoya 464-8601, Japan*

^(f)*Kobayashi-Maskawa Institute for the Origin of Particles and the Universe, Nagoya University, Nagoya 464-8602, Japan*

Abstract

Recently, it was pointed out that the electron and muon $g - 2$ discrepancies can be explained simultaneously by a single flavor-violating axion-like particle (ALP). We show that the parameter regions favored by the muon $g - 2$ are already excluded by the muonium-antimuonium oscillation bound. In contrast, those for the electron $g - 2$ can be consistent with this bound when the ALP is heavier than 1.5 GeV. We propose to search for a signature of the same-sign and same-flavor lepton pairs and the forward-backward muon asymmetry to test the model at the Belle II experiment.

KEYWORDS: Electron $g - 2$, Muon $g - 2$, Axion-like particle, Belle II experiment

1 Introduction

A long-standing discrepancy between the experimental result and the Standard Model (SM) prediction of the anomalous magnetic dipole moment of the muon, $(g - 2)_\mu$, may be a signal of new physics beyond the SM (BSM). Experimentally, it has been determined precisely by the Brookhaven E821 experiment [1–3]. (See Ref. [4] for the latest result updating the value of the muon-to-proton magnetic ratio.) By virtue of dedicated theoretical efforts [5–15], the latest result of $a_\mu \equiv (g - 2)_\mu/2$ is obtained as

$$\Delta a_\mu = a_\mu^{\text{exp}} - a_\mu^{\text{SM}} = \begin{cases} (27.8 \pm 7.4) \times 10^{-10} & [13], \\ (26.1 \pm 7.9) \times 10^{-10} & [12], \end{cases} \quad (1.1)$$

depending particularly on the determination of the hadronic vacuum polarization. They correspond to 3.8 and 3.3 σ discrepancies, respectively. Currently, a new measurement of a_μ is in progress at the Fermilab [16, 17], aiming to reduce the experimental uncertainty by a factor of 4 compared to the Brookhaven result. Another experiment is planned at the J-PARC [18, 19], where distinct methods are employed to measure a_μ .

Recently, a new candidate for the BSM signal has been reported in the electron $g - 2$, $(g - 2)_e$. The fine-structure constant was determined precisely by measuring the caesium mass [20]. Consequently, the theoretical uncertainty of a_e was reduced by a factor of 3 compared to the previous result based on the measurement of the rubidium mass [21]. It revealed that the experimental result [22] deviates from the SM prediction [6] (cf. Ref. [7]) as

$$\Delta a_e = a_e^{\text{exp}} - a_e^{\text{SM}} = (-0.88 \pm 0.36) \times 10^{-12}, \quad (1.2)$$

corresponding to a 2.5 σ discrepancy.

It is noticed that the experimental value of a_e is *smaller* than the SM prediction. This is in contrast to the result of a_μ , where the experimental value is *larger* than the SM one. Although it is not difficult to explain either one of the $g - 2$ anomalies by BSM models, it is challenging to explain both of them simultaneously by a single model because of this sign difference. Furthermore, magnitude of the electron $g - 2$ discrepancy is large: If Δa_μ is explained by a BSM model, the electron $g - 2$ is expected to receive a contribution from this model of $\sim m_e^2/m_\mu^2 \times \Delta a_\mu = \mathcal{O}(10^{-13})$, because the BSM contributions are proportional to the lepton mass squared in a wide class of models. It is obvious that $\mathcal{O}(10^{-13})$ is too small to saturate the discrepancy in Eq. (1.2). Therefore, an additional mechanism, which breaks the lepton mass squared scaling, is required to enhance the contribution to the electron $g - 2$ [?].

In literature, many BSM models have been proposed to explain the anomalies simultaneously [?, 23–32]. In particular, an axion-like particle (ALP) with lepton-flavor violating (LFV) interactions was introduced recently [31, 32].^{#1} Although the ALP is likely to have

^{#1}To explain the mass hierarchy and mixing matrices of the matter fermions, flavor symmetries (horizontal symmetries) are often introduced. Flavor-violating ALPs have been originally proposed as a pseudo-Nambu-Goldstone boson connected with the spontaneous flavor symmetries breaking at a high scale [?, 33–37], and are called flavons or familons.

small couplings, it is expected to be light, and thus, its contribution to the $g - 2$ can be large. The sign difference between Δa_e and Δa_μ is accommodated if axial-vector couplings are larger than vector ones. Besides, the LFV couplings of the ALP enable us to enhance the contribution to the electron $g - 2$ due to a chirality enhancement.

In this paper, we study a unique LFV ALP model which can accommodate the electron and muon $g - 2$ anomalies.^{#2} Since the ALP is a real scalar field, its couplings to the electron and muon induce the transition of the muonium into antimuonium. It will be shown that the parameter regions which explain both of the $g - 2$ anomalies are already excluded by this process. In particular, the ALP contributions to the muon $g - 2$ are tightly constrained. In contrast, those to the electron $g - 2$ can be consistent with it. We will study future prospects of the Belle II experiment to probe such parameter regions. In this paper, the following signatures are evaluated; (1) a production of the same-sign and same-flavor lepton pairs, $e^+e^- \rightarrow \mu^\pm\mu^\pm e^\mp e^\mp$ via an on-shell ALP production, and (2) a forward-backward (FB) asymmetry in muon pair production, $e^+e^- \rightarrow \mu^+\mu^-$.

This paper is organized as follows. In Sec. 2, we briefly introduce a flavor-violating ALP model. In Sec. 3, the ALP contributions to the electron and muon $g - 2$ are explained, and the bound of the muonium-antimuonium oscillation is examined in Sec. 4. Future prospects at the Belle II experiment are investigated in Sec. 5: In Sec. 5.1, a signature of the on-shell production of the ALP is studied, and the FB asymmetry of the muon is discussed in Sec. 5.2. Finally, Sec. 6 is devoted to conclusions and discussion. In Appendix A, the ALP contribution to the transition probability of the muonium into antimuonium is derived, and an analytic formula of the FB asymmetry is provided in Appendix B.

2 Flavor-violating ALP model

Let us introduce ALP (a), which is a real (pseudo-) scalar field, with flavor-violating interactions. Since such an ALP is regarded as a pseudo-Nambu-Goldstone boson of a broken symmetry, the mass m_a becomes naturally small compared to the broken scale Λ . The low-energy effective Lagrangian is obtained as [31, 32, 39]

$$\mathcal{L}_{\text{eff}} = \frac{1}{2} [(\partial_\mu a)^2 - m_a^2 a^2] - \frac{\partial_\mu a}{\Lambda} \sum_{i,j} \bar{f}_i \gamma^\mu (v_{ij} - a_{ij} \gamma_5) f_j + c_{\gamma\gamma}^{\text{eff}} \frac{\alpha}{4\pi} \frac{a}{\Lambda} F_{\mu\nu} \tilde{F}^{\mu\nu} + c_{gg}^{\text{eff}} \frac{\alpha_s}{4\pi} \frac{a}{\Lambda} G_{\mu\nu} \tilde{G}^{\mu\nu}, \quad (2.1)$$

up to dimension-five operators. Here, v_{ij} , a_{ij} , $c_{\gamma\gamma}^{\text{eff}}$ and c_{gg}^{eff} are dimensionless parameters, which depend on details of the UV models. In particular, v_{ij} and a_{ij} are Hermitian matrices with flavor indices i, j . Here, f_i denotes a matter fermion including the lepton in the i -th generation in the mass basis.

For the flavor-conserving interaction ($i = j$), it is noticed that contributions of v_{ii} vanish automatically and only the pseudo-scalar term is left. This is obvious if we consider a case

^{#2}See also Refs. [32, 38] for phenomenology of general flavor-violating ALP models.

when the ALP couples to on-shell fermions. Then, the $a\bar{f}_i f_j$ interaction is rewritten as

$$\mathcal{L}_{\text{eff}} = i\frac{a}{\Lambda} \sum_{i,j} \bar{f}_i [(m_i - m_j)v_{ij} - (m_i + m_j)a_{ij}\gamma_5] f_j, \quad (2.2)$$

by using the equation of motion, where m_i is the mass of f_i . For $i = j$, the coefficient of v_{ii} is found to be zero. Note that $c_{\gamma\gamma}^{\text{eff}}$ and c_{gg}^{eff} are induced generally by fermion one-loop diagrams as $c_{\gamma\gamma}^{\text{eff}}, c_{gg}^{\text{eff}} = \mathcal{O}(a_{ii})$, even if they are suppressed in a high energy scale [31, 40].

In this paper, the ALP interactions are assumed to satisfy

$$|v_{e\mu}, |a_{e\mu}| \gg |v_{e\tau}, |a_{e\tau}|, |v_{\mu\tau}, |a_{\mu\tau}| \gg |a_{ii}|, |c_{\gamma\gamma}^{\text{eff}}|, |c_{gg}^{\text{eff}}|, \quad (2.3)$$

to evade severe constraints from LFV observables.^{#3} The second inequality is imposed because $v_{e\mu}, a_{e\mu}$ can induce LFV decays of muons such as $\mu \rightarrow e\gamma, \pi \rightarrow e\mu, \mu \rightarrow eee$, and $\mu \rightarrow e + \text{invisible}$ when combined with $a_{ii}, c_{\gamma\gamma}^{\text{eff}}$ or c_{gg}^{eff} [31, 32, 41]. On the other hand, the first condition is required because other types of LFV decays such as $\tau \rightarrow \mu\gamma, \tau \rightarrow e\gamma, \tau \rightarrow \mu\mu e$, and $\tau \rightarrow \mu ee$ can be generated by combining $v_{e\mu}, a_{e\mu}$ with those including the tau lepton [32, 41]. Such a hierarchy between the ALP interactions could be obtained from Z_4 lepton flavor symmetry (cf. Ref. [42]).

From Eq. (2.1), it is noticed that v_{ij} and a_{ij} appear in associated with Λ in the expressions of ALP contributions to observables. It is convenient to define dimensionless scalar coupling $(y_V)_{e\mu}$ and pseudo-scalar coupling $(y_A)_{e\mu}$ as^{#4}

$$(y_V)_{e\mu} = -i\frac{m_\mu}{\Lambda}v_{e\mu}, \quad (y_A)_{e\mu} = -i\frac{m_\mu}{\Lambda}a_{e\mu}. \quad (2.4)$$

For instance, by neglecting the electron mass, the interactions (2.2) are expressed as

$$\begin{aligned} \mathcal{L}_{\text{eff}} &\simeq -i\frac{m_\mu}{\Lambda}a\bar{e}(v_{e\mu} + a_{e\mu}\gamma_5)\mu + i\frac{m_\mu}{\Lambda}a\bar{\mu}(v_{e\mu}^* - a_{e\mu}^*\gamma_5)e \\ &= (y_V)_{e\mu}a\bar{e}\mu + (y_A)_{e\mu}a\bar{e}\gamma_5\mu + \text{H.c.} \end{aligned} \quad (2.5)$$

Note that $v_{\mu e} = v_{e\mu}^*$ and $a_{\mu e} = a_{e\mu}^*$ by Hermiticity. Therefore, the ALP contributions are represented by the following parameters,

$$m_a, \quad (y_V)_{e\mu}, \quad (y_A)_{e\mu}. \quad (2.6)$$

Note that the partial wave unitarity sets the upper bound [32]:

$$\left| (y_{V,A})_{e\mu} \right| \lesssim 2\sqrt{\frac{2\pi}{3}} \simeq 2.9. \quad (2.7)$$

^{#3}We ignore ALP interactions with quarks because they are irrelevant for the lepton $g-2$. The interactions with neutrinos are also irrelevant in the following analysis.

^{#4}The couplings y_V and y_A are related to those in Ref. [31] as

$$(y_V)_{e\mu} = i\frac{m_\mu}{f} \frac{(k_e + k_E)_{e\mu}}{2}, \quad (y_A)_{e\mu} = -i\frac{m_\mu}{f} \frac{(k_e - k_E)_{e\mu}}{2}.$$

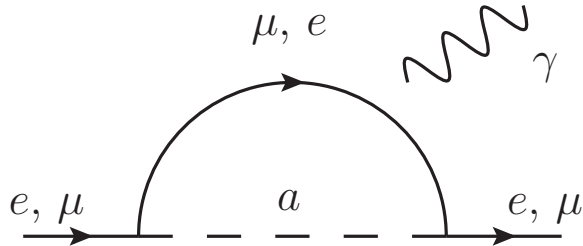


Figure 1. Feynman diagram for the ALP contributions to the electron and muon $g - 2$. Contributions from $a\gamma\gamma$ and flavor-diagonal ALP interactions are assumed to be suppressed.

3 Lepton $g - 2$

The ALP contributions to the lepton $g - 2$ are generated at the one-loop level as displayed in Fig. 1. From the effective Lagrangian in Eq. (2.1), we obtain the results as,^{#5}

$$a_e^{\text{ALP}} = -\frac{1}{16\pi^2} \frac{m_e}{m_\mu} \left\{ |(y_A)_{e\mu}|^2 - |(y_V)_{e\mu}|^2 \right\} \left[\frac{2x_a^2 \log x_a}{(x_a - 1)^3} + \frac{1 - 3x_a}{(x_a - 1)^2} \right], \quad (3.1)$$

$$a_\mu^{\text{ALP}} = \frac{1}{16\pi^2} \left\{ |(y_A)_{e\mu}|^2 + |(y_V)_{e\mu}|^2 \right\} \left[2x_a^2 \log \left(\frac{x_a}{x_a - 1} \right) - 1 - 2x_a \right], \quad (3.2)$$

for $m_e^2 \ll m_\mu^2, m_a^2$, where $x_a = m_a^2/m_\mu^2$. These results are consistent with those in Refs. [31, 32].^{#6} Although a_μ^{ALP} seems to diverge at $x_a = 1$, this is because the approximation becomes invalid; at $x_a = 1$, the result becomes

$$a_\mu^{\text{ALP}}|_{x_a=1} = \frac{1}{16\pi^2} \left\{ |(y_A)_{e\mu}|^2 + |(y_V)_{e\mu}|^2 \right\} \left[\log \left(\frac{m_\mu^2}{m_e^2} \right) - 3 \right], \quad (3.3)$$

for $m_e^2 \ll m_\mu^2$. As pointed out in Ref. [31], the sign of a_e^{ALP} can be opposite to that of a_μ^{ALP} particularly when $|(y_A)_{e\mu}| > |(y_V)_{e\mu}|$ is satisfied. In fact, the loop function in a_e^{ALP} is positive for any x_a , while the function in a_μ^{ALP} is positive when $x_a \gtrsim 0.9$.

For $|(y_A)_{e\mu}| \gg |(y_V)_{e\mu}|$ with $x_a \sim 1$, the ALP contributions are scaled as

$$a_e^{\text{ALP}} \sim -\frac{m_e}{m_\mu} a_\mu^{\text{ALP}}. \quad (3.4)$$

This result is understood as follows: the definition of the anomalous magnetic moment a_ℓ is normalized by the lepton mass m_ℓ and requires a chirality flip for the lepton. In the ALP

^{#5}In this paper, we focus on the flavor-violating ALP contributions. However, it was argued that the electron and muon $g - 2$ discrepancies can also be explained simultaneously by large flavor-conserving ALP couplings as $|c_{\gamma\gamma}^{\text{eff}}| \gg |a_{\mu\mu}| \gg |v_{ij}|, |a_{ij}|_{i \neq j}$ [31, 32].

^{#6}For a model with the flavor-violating Yukawa interactions (2.5), the muon $g - 2$ was studied in Ref. [43] with providing the exact formula, and its relation to the electron $g - 2$ was discussed in Ref. [44].

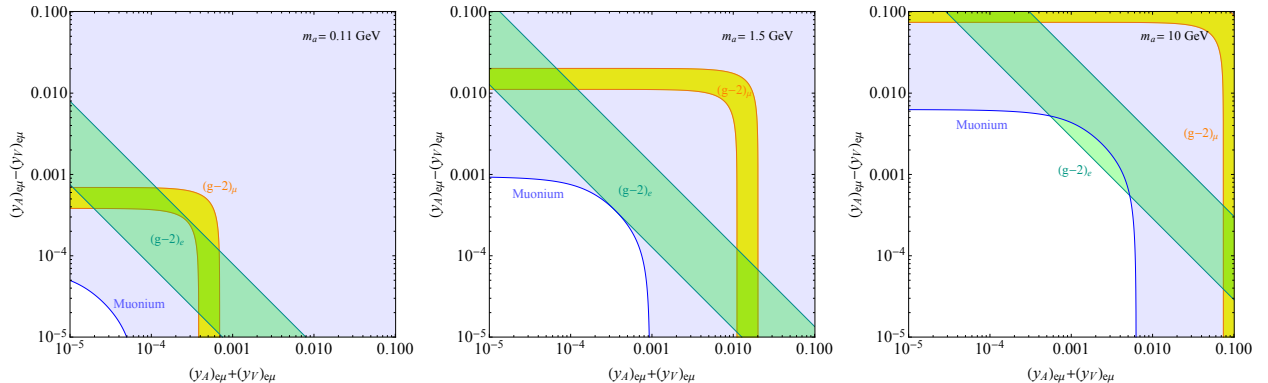


Figure 2. Δa_e and Δa_μ are explained in the green and yellow regions within the 2σ level, respectively, for $m_a = 110$ MeV (left), $m_a = 1.5$ GeV (middle) and $m_a = 10$ GeV (right). The blue-shaded regions are excluded by the muonium-antimuonium oscillation bound at the 90% CL.

contributions (see Fig. 1), the latter for the electron $g - 2$ is caused by the intermediate muon, while it is provided by the external muon for the muon $g - 2$. Thus, the ratio is scaled by the single power of the lepton mass. Then, if the ALP contribution to the muon $g - 2$ is comparable to Δa_μ , the contribution to the electron $g - 2$ becomes as large as $\mathcal{O}(10^{-11})$, which overshoots Δa_e in Eq. (1.2) by an order of magnitude. Therefore, to explain the anomalies simultaneously, a parameter tuning is necessary between $|(y_V)_{e\mu}|$ and $|(y_A)_{e\mu}|$ at an order of 1–10% levels, depending on m_a .

In Fig. 2, the $g - 2$ favored regions are shown for $m_a = 110$ MeV (left), 1.5 GeV (middle) and 10 GeV (right). The discrepancies of $(g-2)_e$ and $(g-2)_\mu$ are explained within the 2σ level in the green and yellow regions, respectively. Here and hereafter, $\Delta a_\mu = (27.8 \pm 7.4) \times 10^{-10}$ [13] is adopted. It is found that both anomalies can be reconciled by a mild tuning between $(y_V)_{e\mu}$ and $(y_A)_{e\mu}$ when the ALP is light, while the parameter tuning becomes tighter for larger m_a , as mentioned in Ref. [31]. In the figures, we also show the exclusion limit from the muonium-antimuonium oscillation measurement by the blue-shaded regions, which will be discussed in the next section.

When m_a is smaller than $(m_\mu - m_e)$, the decay of $\mu \rightarrow ea$ is kinematically open and tightly constrained by a search for $\mu \rightarrow e + \text{invisible}$ [31, 32, 45]. Hence, no parameter space is available in $m_a < (m_\mu - m_e)$ to explain both of the anomalies.

Finally, let us comment on CP -violating contributions from the flavor-violating ALP couplings. The most severe constraint comes from the electric dipole moment (EDM) of the electron, $|d_e| < 1.1 \times 10^{-29}$ e cm (90% CL) [46]. The contribution is generated by a similar diagram as Fig. 1, but the contribution is proportional to $\text{Im} [(y_V)_{e\mu}(y_A)_{e\mu}^*]$. Naively, it is estimated as $|d_e| \sim e/(2m_e)a_e^{\text{ALP}} \sim \mathcal{O}(10^{-23})$ e cm, by requiring $a_e^{\text{ALP}} \sim \Delta a_e$. Therefore, the ALP couplings are required to satisfy $\text{Im} [(y_V)_{e\mu}(y_A)_{e\mu}^*] < 10^{-6} [|(y_A)_{e\mu}|^2 - |(y_V)_{e\mu}|^2]$.

4 Muonium-antimuonium oscillation

Since the ALP is a real scalar boson, an exchange of the flavor-violating ALP generates effective $[\bar{\mu}e][\bar{\mu}e]$ -type operators in a low-energy scale. Such operators can be probed by measurements of a transition of a muonium ($M = \mu^+e^-$) into an antimuonium ($\bar{M} = \mu^-e^+$), which is so-called the muonium-antimuonium (M - \bar{M}) oscillation [47–49]. Since the SM prediction is highly suppressed by the neutrino masses [50], it is very sensitive to the $e\mu$ flavor-violating interactions.

According to Refs. [51–53], we obtain the M - \bar{M} transition probability within the effective Lagrangian in Eq. (2.5) as

$$P_{M\bar{M}} = \frac{8}{\pi^2 a_B^6 \lambda^2 m_a^4} \left[|c_{0,0}|^2 \left| (y_V)_{e\mu}^2 - \left(1 + \frac{1}{\sqrt{1+X^2}} \right) (y_A)_{e\mu}^2 \right|^2 + |c_{1,0}|^2 \left| (y_V)_{e\mu}^2 - \left(1 - \frac{1}{\sqrt{1+X^2}} \right) (y_A)_{e\mu}^2 \right|^2 \right], \quad (4.1)$$

where $\lambda = 3.00 \times 10^{-19} \text{ GeV}$ and $a_B = 2.69 \times 10^5 (\text{GeV})^{-1}$. The factor X in the right-handed side parametrizes effects of the external magnetic field B as $X = 6.31B (\text{Tesla})^{-1}$. The derivation is provided in Appendix A. Note that this formula is obtained by integrating out the intermediate ALP, *i.e.*, valid for $m_a > m_\mu$. We also assumed the CP symmetry, and thus, parity-violating interferences between the scalar and pseudo-scalar interactions are dropped [54].

The most precise measurement has been performed by the MACS experiment at PSI [55]. The upper bound on the M - \bar{M} oscillation was obtained as

$$P_{M\bar{M}} < 8.3 \times 10^{-11}, \quad (4.2)$$

at the 90% CL. In the experiment, the external magnetic field of $B = 0.1 \text{ Tesla}$ was applied to detect an energetic e^- from the antimuonium decay in a magnetic spectrometer. Besides, c_{F,m_F} stands for a population of the muonium state in the experimental setup where F is the total angular momentum of the muonium and $m_F = -F, -F+1, \dots, F$. For the MACS experiment, it is estimated as $|c_{0,0}|^2 = 0.32$ and $|c_{1,0}|^2 = 0.18$ [51, 52].^{#7} For specific cases, we obtain the upper bounds,^{#8}

$$\left| (y_V)_{e\mu} \right| < 2.9 \times 10^{-4} \left(\frac{m_a}{\text{GeV}} \right), \quad \text{for } (y_A)_{e\mu} = 0, \quad (4.3)$$

$$\left| (y_A)_{e\mu} \right| < 2.4 \times 10^{-4} \left(\frac{m_a}{\text{GeV}} \right), \quad \text{for } (y_V)_{e\mu} = 0, \quad (4.4)$$

$$\left| (y_V)_{e\mu} \right| < 3.1 \times 10^{-4} \left(\frac{m_a}{\text{GeV}} \right), \quad \text{for } (y_V)_{e\mu} = (y_A)_{e\mu}. \quad (4.5)$$

^{#7}As a crosscheck, we reproduced magnetic field correction factors S_B in Table II in Ref. [55] by supposing an equal population, $|c_{0,0}|^2 = |c_{1,-1}|^2 = |c_{1,0}|^2 = |c_{1,1}|^2 = 0.25$.

^{#8}These bounds are consistent with those in Refs. [41, 56], where the magnetic effects are taken into account via S_B . Also, our results are slightly severer than those in Refs. [57, 58].

In Fig. 2, the blue-shaded regions are excluded by the $M-\bar{M}$ oscillation. It is shown that the region favored by the muon $g-2$ is completely excluded.^{#9} Since both of the ALP contributions to a_μ and $P_{M\bar{M}}$ are scaled by $(y_{V,A})^2/m_a^2$ for $m_a \gg m_\mu$, Δa_μ cannot be explained even by a heavier ALP. On the other hand, Δa_e can be explained for $m_a > 1.5$ GeV. Since the loop function of the ALP contribution to a_e is proportional to $\log(m_a^2/m_\mu^2)/m_a^2$ for $m_a \gg m_\mu$, it is likely to be amplified compared to that for a_μ , and the constraint from the $M-\bar{M}$ oscillation becomes relaxed. In the next section, we will study how to search for such an ALP at the Belle II experiment.

5 Collider signals at Belle II

In this section, we investigate experimental sensitivities to the $e\mu$ flavor-violating ALP at the Belle II experiment. First, we consider a process $e^+e^- \rightarrow \mu^\pm e^\mp a \rightarrow \mu^\pm \mu^\pm e^\mp e^\mp$, which is effective for $m_a \leq \sqrt{s_{\text{BelleII}}}$, where $\sqrt{s_{\text{BelleII}}} = 10.58$ GeV is the center-of-mass energy of the experiment. Next, the FB asymmetry in the process $e^+e^- \rightarrow \mu^+\mu^-$ is investigated, where an off-shell ALP contributes, and thus, the observable has sensitivity to the ALP for $m_a \geq \sqrt{s_{\text{BelleII}}}$.

5.1 $e^+e^- \rightarrow \mu^\pm \mu^\pm e^\mp e^\mp$ via on-shell ALP

In the $e\mu$ flavor-violating ALP model, productions of the same-sign and same-flavor leptons pairs can proceed,^{#10}

$$e^+e^- \rightarrow \mu^\pm e^\mp a \rightarrow \mu^\pm \mu^\pm e^\mp e^\mp. \quad (5.1)$$

The branching ratios of the ALP is $\text{BR}(a \rightarrow \mu^+e^-) = \text{BR}(a \rightarrow \mu^-e^+) = 0.5$ for $m_a \geq m_\mu + m_e$. In Fig. 3, we show some of the diagrams which contribute to the process. In the left and middle diagrams, an on-shell ALP is produced, while it is exchanged in an off-shell state in the right diagram.^{#11}

This process is quite unique; the final state includes two pairs of the same-sign electrons and muons. Such same-flavor and same-sign leptons processes are never produced within the SM. Besides, the charge reconstruction of leptons is quite accurate in Belle II experiment [59–61]. Hence, we simply neglect the SM background in the following analysis.^{#12}

^{#9}The same conclusion was made in Ref. [41] for a light scalar model with effective Yukawa couplings.

^{#10}A process $e^+e^- \rightarrow \mu^\pm e^\mp a \rightarrow \mu^\pm \mu^\mp e^\pm e^\mp$ is also predicted but less distinctive due to larger backgrounds.

^{#11}In the analysis, although the off-shell contributions are included, we checked that the production cross section is dominated by the on-shell ALP productions. Besides, ALP pair production, $e^+e^- \rightarrow aa \rightarrow \mu^\pm \mu^\pm e^\mp e^\mp$, is included in our analysis, and we found that its contribution is negligible in Figs. 4 and 5.

^{#12}Another distinctive feature of the signal is an invariant mass peak around the ALP mass, $(p_e + p_\mu)^2 = m_a^2$. Although there are two possible combinations to construct the $e\mu$ resonance, the wrong combination just provides a continuum distribution. To obtain a clear peak, we further need to drop it on event-by-event basis as discussed in Sec 3.3.1 of Ref. [62]. In this paper, we do not impose this condition.

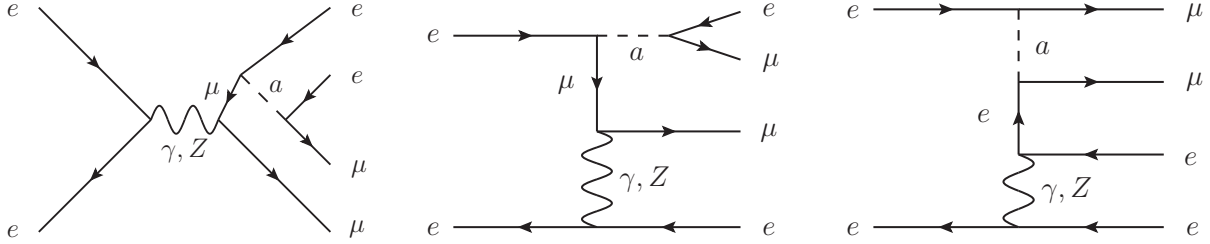


Figure 3. Examples of Feynman diagrams for $e^+e^- \rightarrow \mu^\pm\mu^\pm e^\mp e^\mp$.

The fiducial production cross section is estimated by using **MadGraph5** [63] with the ALP model file generated by **FeynRules** [64]. Signal events with the asymmetric beam energy $E(e^-) = 7 \text{ GeV}$ and $E(e^+) = 4 \text{ GeV}$ [61], are generated, and the following kinematical cuts for the final state leptons are imposed in the laboratory frame [60, 61]:

$$e : 12^\circ \leq \theta \leq 155^\circ, \quad |\vec{p}_e| \geq 0.02 \text{ GeV}, \quad (5.2)$$

$$\mu : 25^\circ \leq \theta \leq 145^\circ, \quad |\vec{p}_\mu| \geq 0.6 \text{ GeV}, \quad (5.3)$$

where θ is an angle to the e^- beam line in the laboratory frame. Besides, the electron and muon tagging efficiencies are taken into account for each final-state lepton by following Ref. [61]; they depend on the electron/muon energy but are assumed to be independent of the polar and azimuthal angles for simplicity.

Figure 4 shows the fiducial cross section after the kinematical cuts as a function of the ALP mass. Here, $(y_A)_{e\mu}$ and m_a are varied with $(y_V)_{e\mu} = 0$ fixed.^{#13} The green band represents a predicted cross section in which the electron $g - 2$ discrepancy is explained within the 2σ level, and the green dashed line stands for the central value of the discrepancy. The horizontal dotted, dashed, and solid blue lines represent the expected sensitivities of the Belle II experiment with the integrated luminosity of 1, 5, and 50 ab^{-1} , respectively. If no signal events are observed, the region above the horizontal lines will be excluded at 95% CL, where the Poisson distribution is applied. It is found that when the ALP accounts for the central value of Δa_e , the Belle II experiment with the integrated luminosity of 5 (50) ab^{-1} can test the model for $1.5 \leq m_a \leq 9.8 \text{ GeV}$ ($0.15 \leq m_a \leq 9.9 \text{ GeV}$). In a smaller mass region, the muon emitted by the ALP decay becomes soft and cannot pass the kinematical cut in Eq. (5.3). On the other hand, the production cross section of $e^+e^- \rightarrow \mu^\pm e^\mp a$ for a heavier ALP is suppressed both by the phase space and by the kinematical cuts.

Let us comment on a case with $m_a \gtrsim \sqrt{s_{\text{BelleII}}}$. Although the on-shell production of a is kinematically forbidden, the off-shell processes are still allowed. However, since the production cross section becomes very small in the parameter region where the electron $g - 2$ discrepancy is explained, the ALP model will not be probed by the Belle II experiment via $e^+e^- \rightarrow \mu^\pm\mu^\pm e^\mp e^\mp$.^{#14}

^{#13}When $(y_V)_{e\mu} \neq 0$, larger couplings are required to explain Δa_e because of the cancellation in Eq. (3.1). Then, larger cross sections are predicted and the model can be tested with smaller luminosity.

^{#14}Recently, LHC sensitivities to the flavor-violating ALP were studied by Ref. [58] in a process of $pp \rightarrow$

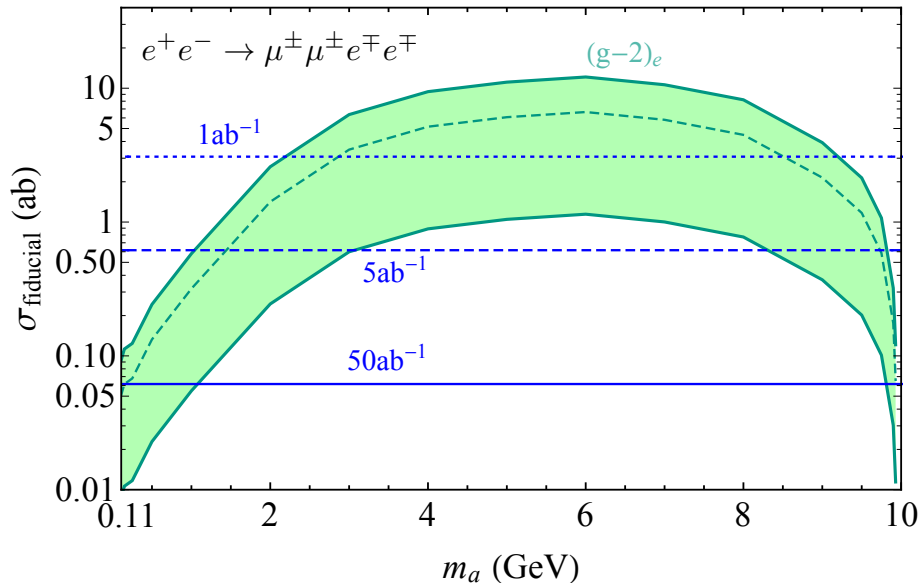


Figure 4. The fiducial production cross section of $e^+e^- \rightarrow \mu^\pm\mu^\pm e^\mp e^\mp$ as a function of m_a . Here, $(y_A)_{e\mu}$ and m_a are varied, while $(y_V)_{e\mu} = 0$ is fixed. The electron $g - 2$ discrepancy is explained within the 2σ level in the green band with the central value shown by the green dashed line. The horizontal dotted, dashed, and solid blue lines represent the expected sensitivity of the Belle II experiment with the integrated luminosity of 1, 5, and 50 ab^{-1} , respectively.

5.2 Forward-backward asymmetry of $e^+e^- \rightarrow \mu^+\mu^-$

Next, we consider the FB asymmetry of $e^+e^- \rightarrow \mu^+\mu^-$. Within the SM, it occurs by an interference of s -channel γ and Z exchanges at the tree level. Since the latter contribution is suppressed by a factor of $s_{\text{BelleII}}/m_Z^2 \ll 1$, the SM value becomes tiny at the Belle II experiment [65, 66]. On the other hand, the flavor-violating ALP contributes in a t -channel process. Such a contribution can modify an angular distribution of the muon pair and be probed by measuring the FB asymmetry:

$$A_{\text{FB}} = \frac{N^+(\cos\theta^* > 0) - N^+(\cos\theta^* < 0)}{N^+(\cos\theta^* > 0) + N^+(\cos\theta^* < 0)}, \quad (5.4)$$

where θ^* is an angle between μ^+ and e^+ in the center-of-mass frame and $N^+(\cos\theta^* > 0)$ is the number of μ^+ satisfying $\cos\theta^* > 0$.

The ALP contribution to the FB asymmetry is evaluated by calculating an interference of the transition amplitudes of the SM and ALP contributions to the production cross section. Since the SM amplitude is dominated by the s -channel γ contribution, we obtain the

$h \rightarrow \mu^\pm\mu^\pm e^\mp e^\mp$. It was shown that the region of $20 \lesssim m_a \lesssim 80 \text{ GeV}$ can be probed accurately and its sensitivity is better than the M-M oscillation. Future lepton-collider sensitivities were also discussed in Ref. [41].

interference term \mathcal{I} as

$$\mathcal{I} = \frac{e^2}{2(k^2 - m_a^2)} \left[\left| (y_V)_{e\mu} \right|^2 + \left| (y_A)_{e\mu} \right|^2 \right] \times \left[s(1 + \cos^2 \theta^*) + 4m_\mu^2(1 - \cos^2 \theta^*) - 4\sqrt{s \left(\frac{s}{4} - m_\mu^2 \right)} \cos \theta^* \right], \quad (5.5)$$

where $s = s_{\text{BelleII}}$ and k is a momentum transfer of the ALP,

$$k^2 = m_\mu^2 - \frac{s}{2} + \sqrt{s \left(\frac{s}{4} - m_\mu^2 \right)} \cos \theta^*. \quad (5.6)$$

The derivation is provided in Appendix B. Consequently, the ALP contribution to the FB asymmetry is given as

$$A_{\text{FB}}^{\text{ALP}} = \frac{3}{8e^4} \left(\int_0^1 d(\cos \theta^*) \mathcal{I} - \int_{-1}^0 d(\cos \theta^*) \mathcal{I} \right). \quad (5.7)$$

When $|(y_A)_{e\mu}| \gg |(y_V)_{e\mu}|$ and $m_a^2 \gg s$, it is approximated as

$$A_{\text{FB}}^{\text{ALP}} \simeq \frac{3}{32\pi\alpha} \left| (y_A)_{e\mu} \right|^2 \frac{s}{m_a^2}. \quad (5.8)$$

If the Belle II experiment is supposed to detect $A_{\text{FB}}^{\text{ALP}} > \delta A_{\text{FB}}$ in future, the ALP coupling

$$\left| (y_A)_{e\mu} \right| > 4.8 \times 10^{-2} \sqrt{\delta A_{\text{FB}}} \left(\frac{m_a}{\text{GeV}} \right), \quad (5.9)$$

could be probed for $|(y_A)_{e\mu}| \gg |(y_V)_{e\mu}|$ and $m_a^2 \gg s_{\text{BelleII}}$.

The Belle II experiment may achieve a statistical uncertainty of $\delta A_{\text{FB}} \sim 10^{-5}$ with the integrated luminosity of 50 ab^{-1} [65], though the systematic uncertainty is still unknown. On the other hand, the uncertainty of the SM prediction is likely to be dominated by that of the vacuum polarization.^{#15} Its size is inferred to be as large as or slightly larger than the experimental statistical uncertainty by considering an analogy to a study of the FB asymmetry in the electroweak precision test (see, *e.g.*, Ref. [67] for a recent work). Thus, reductions of the SM uncertainties could be essential to improve the Belle II sensitivity. See Refs. [68, 69] for prospects of the vacuum polarization contribution.

In this paper, we consider $\delta A_{\text{FB}} = 10^{-4}$ and 10^{-5} for the future sensitivity as a reference. In order to investigate the ALP contribution to the FB asymmetry at these accuracies, one needs $\mathcal{O}(10^{8-10})$ event samples for the Monte Carlo simulation. This is beyond the scope of this paper and we compare Eq. (5.7) with δA_{FB} to derive the future sensitivity. Note that although signal acceptance and efficiencies should be taken into account, we have checked

^{#15}Although uncertainties from long-distance QED corrections could also be large, they might be suppressed by investigating $\mu^+\mu^-$ angular distributions thanks to high statistics at the Belle II experiment [66].

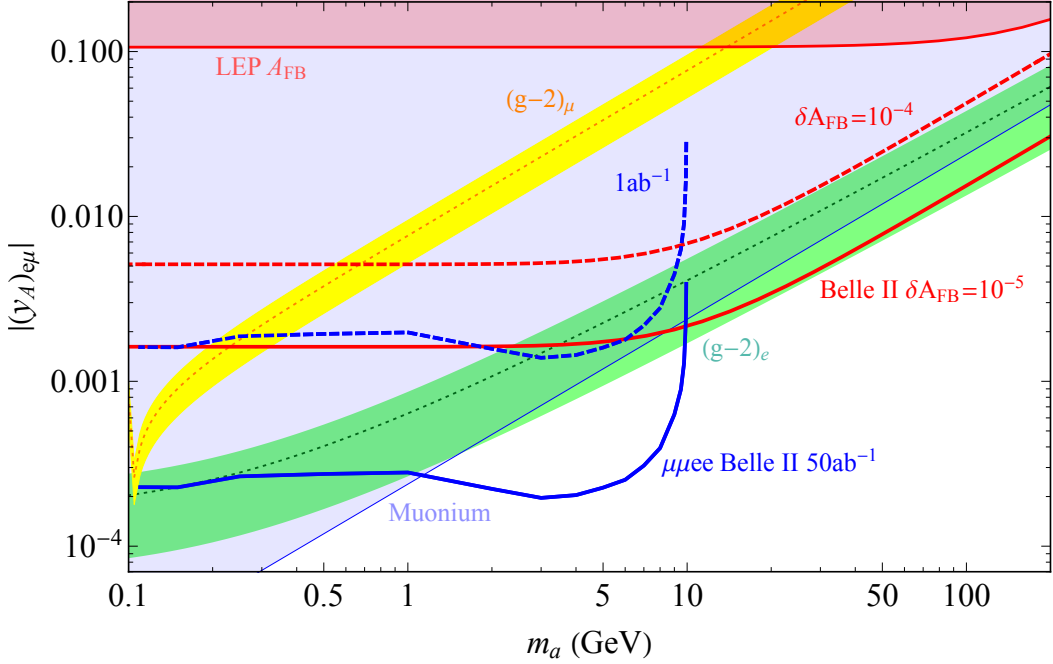


Figure 5. The Belle II sensitivities are shown with $(y_V)_{e\mu} = 0$ fixed. The dashed and solid red lines represent the sensitivity of the A_{FB} measurement with resolutions of $\delta A_{\text{FB}} = 10^{-4}$ and 10^{-5} , respectively. The dashed and solid blue lines represent the sensitivity of searching for $e^+e^- \rightarrow \mu^\pm\mu^\pm e^\mp e^\mp$ with the integrated luminosity of 1 and 50 ab^{-1} , respectively. In the green and yellow regions, Δa_e and Δa_μ are explained within the 2σ level with the central value drawn by the green and orange dotted lines, respectively. The blue-shaded region is excluded by the $M-\bar{M}$ oscillation at the 90% CL. The red-shaded region is excluded by the LEP measurement of A_{FB} .

that such corrections are minor; the event number may be reduced by $\sim 10\%$. We neglect them in the analysis for simplicity.

In Fig. 5, the Belle II sensitivity to the FB asymmetry is shown for $\delta A_{\text{FB}} = 10^{-4}$ and 10^{-5} by the dashed and solid red lines, respectively. Here, $(y_V)_{e\mu} = 0$ is fixed. In the green and yellow regions, Δa_e and Δa_μ are explained within the 2σ level with the central value drawn by the green and orange dotted lines, respectively. The $M-\bar{M}$ oscillation excludes the blue-shaded region at the 90% CL. It is seen that the region favored by the muon $g-2$ is completely excluded by the $M-\bar{M}$ oscillation. In contrast, although Δa_e can be explained with satisfying the $M-\bar{M}$ oscillation bound, it is found that the Belle II measurement of the FB asymmetry with $\delta A_{\text{FB}} = 10^{-5}$ can probe most of such parameter regions for $m_a \gtrsim 9 \text{ GeV}$.

The LEP experiment also performed measurements of the FB asymmetry of $e^+e^- \rightarrow \mu^+\mu^-$ for the center-of-mass energies from 130 GeV to 207 GeV [70]. The experimental uncertainties are dominated by the statistical one, and one of the most precise results is

provided at $\sqrt{s} = 207 \text{ GeV}$ as

$$A_{\text{FB}}^{\text{LEP}} = 0.535 \pm 0.028 \pm 0.004, \quad (5.10)$$

where the first and second errors are statistical and systematic uncertainties, respectively. On the other hand, it is referred to in Ref. [70] that the SM value is 0.552 with the uncertainty smaller than the above statistical error. Since this is consistent with the experimental result, the ALP contribution is constrained by the LEP experiment. In Fig. 5, we show the LEP A_{FB} bound at the 2σ level by the red-shaded region.^{#16} It is found that the LEP measurement does not constrain the parameter region favored by the electron $g - 2$. Although the limit may be improved by combining all the LEP results in various center-of-mass energies, we expect that it is still weaker than the constraint by the $M-\bar{M}$ oscillation and cannot reach the Belle II sensitivities.^{#17}

Finally, in Fig. 5, the Belle II sensitivity to a search for $e^+e^- \rightarrow \mu^\pm e^\mp a \rightarrow \mu^\pm \mu^\pm e^\mp e^\mp$, which was discussed in the last subsection, is also shown for the integrated luminosity of 1 and 50 ab^{-1} by the dashed and solid blue lines, respectively. For $1 \lesssim m_a \lesssim 10 \text{ GeV}$ with 50 ab^{-1} , it is found that the process is useful to probe the parameter region which is favored by the electron $g - 2$ and consistent with the $M-\bar{M}$ oscillation data. This result is complementary to the FB asymmetry; we conclude that the ALP parameter region favored by the electron $g - 2$ could be tested almost entirely by the Belle II experiment.

6 Conclusion

In this paper, we revisited the $e\mu$ flavor-violating ALP model motivated by the electron and muon $g - 2$ anomalies. Such an ALP inevitably induces the muonium-antimuonium oscillation, and it was found that whole the parameter regions which explain both of the discrepancies simultaneously are already excluded.

^{#16}In the analysis, we include the s -channel Z contribution to the SM amplitude as well as that from the γ exchange, though the asymmetry is dominated by the interference of the ALP amplitude with the γ contribution for $\sqrt{s} = 207 \text{ GeV}$.

^{#17}In Ref. [70], constraints for four-fermion interactions are also investigated by combining all the LEP results; according to Table 3.15, one finds $\Lambda > 12.1 \text{ TeV}$ for $A0^-$ model, which corresponds to a purely pseudo-scalar electron-muon interaction. See the reference for definitions of the parameters. Since $(y_A)_{e\mu}$ is related to Λ as $|(y_A)_{e\mu}| = \sqrt{8\pi} m_a / \Lambda$, the limit is converted to be

$$\left| (y_A)_{e\mu} \right| < 0.41 \left(\frac{m_a}{\text{TeV}} \right), \quad (5.11)$$

at the 95% CL, where the ALP is assumed to be decoupled. This result is consistent with Ref. [41]. On the other hand, by using Eq. (5.10) we obtain

$$\left| (y_A)_{e\mu} \right| < 0.57 \left(\frac{m_a}{\text{TeV}} \right), \quad (5.12)$$

for $m_a \gg 207 \text{ GeV}$. Thus, our result relying solely on Eq. (5.10) is not much weaker than the fully combined limit, Eq. (5.11).

Nevertheless, the model can accommodate only the electron $g - 2$ anomaly. In order to test such parameter regions, we investigated the Belle II sensitivity of searching for the on-shell ALP production of $e^+e^- \rightarrow \mu^\pm e^\mp a$ followed by $a \rightarrow \mu^\pm e^\mp$ and the forward-backward asymmetry of $e^+e^- \rightarrow \mu^+\mu^-$. We found that the former provides a good sensitivity for $m_a < 10$ GeV, and the latter does for $m_a > 10$ GeV. Hence, these measurements are complementary and provide better sensitivities than the muonium-antimuonium oscillation bound for $m_a > 1$ GeV. As a result, the parameter region favored by the electron $g - 2$ anomaly can be tested almost entirely by the Belle II experiment with the integrated luminosity of 50 ab^{-1} .

Finally, we briefly comment on a light and flavor-violating complex scalar field. If this complex scalar S carries an electron or muon charge, the low-energy effective interactions become $-(\partial_\mu S/\Lambda)\bar{e}\gamma^\mu(v_{e\mu} - a_{e\mu}\gamma_5)\mu$ or $(y_V)_{e\mu}S\bar{e}\mu + (y_A)_{e\mu}S\bar{e}\gamma_5\mu$ with their Hermitian conjugate, while interactions of $e \leftrightarrow \mu$ are forbidden. Although the contributions to the lepton $g - 2$ become analogous to Eqs. (3.1) and (3.2), the transition of the muonium into antimuonium does not proceed via the scalar. Hence, the flavor-violating complex scalar can explain both $g - 2$ anomalies simultaneously, though the UV completion is nontrivial [58].^{#18#19} At the Belle II experiment, the measurement of the forward-backward asymmetry could probe such a parameter region when $m_S > \mathcal{O}(1)$ GeV; the muon $g - 2$ discrepancy requires larger couplings, which enhance A_{FB} , too. Although the same-flavor and same-sign productions of the electron and muon pairs do never proceed, one can consider a flavor-violating resonant search in the same-flavor and opposite-sign lepton pair productions of $e^+e^- \rightarrow \mu^\pm e^\mp a \rightarrow \mu^\pm e^\mp \mu^\mp e^\pm$, which could be a target in the early stage of the Belle II experiment.

Acknowledgements

We would like to thank Yael Shadmi and Yotam Soreq for worthwhile discussions of the forward-backward asymmetry in the muon pair production. We also thank Iftah Galon, Junji Hisano, Kenji Inami, Akimasa Ishikawa, Kodai Matsuoka, Satoshi Mishima, Tsuzuki Noritsugu, Olcyr Sumensari, Kazuhiro Tobe, and Koji Tsumura for many useful comments and discussions. S.I. would like to thank Michigan State University for its warm hospitality where this project was initiated. The work of S.I. is supported by Kobayashi-Maskawa Institute for the Origin of Particles and the Universe, Toyoaki scholarship foundation and the Japan Society for the Promotion of Science (JSPS) Research Fellowships for Young Scientists, No. 19J10980. This work is supported in part by the Grant-in-Aid for Scientific Research B (No.16H03991 [ME]), and Early-Career Scientists (No.16K17681 [ME] and No.19K14706 [TK]). The work of T.K. is also supported by the Israel Science Foundation (Grant No. 751/19).

^{#18}Note that when the effective interaction is $(y_R)_{e\mu}S\bar{e}P_R\mu + \text{H.c.}$, the contribution to the electron $g - 2$ vanishes, while the muon $g - 2$ anomaly can be explained.

^{#19}Even when there is a mass difference between the scalar and pseudo-scalar components of the complex scalar field, a destructive interference works between their contributions to the muonium-antimuonium oscillation. In particular, when a phase component in the complex scalar corresponds to ALP, its contribution to the oscillation could be diminished by a scalar partner unless its mass is far from the ALP one.

A Muonium-antimuonium transition

In this appendix, a probability of the transition of the muonium ($M = \mu^+e^-$) into antimuonium ($\bar{M} = \mu^-e^+$) is derived under an external magnetic field B . We follow the analysis explored in Ref. [52].

Neglecting effects of the B field, depending on spins of the leptons, there are four types of the $1S$ muonium state $|M; J, m_J\rangle$:

$$|M; 0, 0\rangle_0 = \frac{1}{\sqrt{2}} (-|M; \uparrow, \downarrow\rangle + |M; \downarrow, \uparrow\rangle), \quad (\text{A.1})$$

$$|M; 1, 0\rangle_0 = \frac{1}{\sqrt{2}} (|M; \uparrow, \downarrow\rangle + |M; \downarrow, \uparrow\rangle), \quad (\text{A.2})$$

$$|M; 1, 1\rangle = |M; \uparrow, \uparrow\rangle, \quad |M; 1, -1\rangle = |M; \downarrow, \downarrow\rangle. \quad (\text{A.3})$$

Under the nonzero external B field, they are modified via the magnetic dipole moment of leptons:

$$|M; 0, 0\rangle_B = \frac{c+s}{\sqrt{2}} |M; 0, 0\rangle_0 + \frac{c-s}{\sqrt{2}} |M; 1, 0\rangle_0, \quad (\text{A.4})$$

$$|M; 1, 0\rangle_B = \frac{c+s}{\sqrt{2}} |M; 1, 0\rangle_0 - \frac{c-s}{\sqrt{2}} |M; 0, 0\rangle_0, \quad (\text{A.5})$$

and the $|M; 1, \pm 1\rangle$ states change only their energy levels. Here, s and c are

$$s = \frac{1}{\sqrt{2}} \left[1 - \frac{X}{\sqrt{1+X^2}} \right]^{\frac{1}{2}}, \quad c = \frac{1}{\sqrt{2}} \left[1 + \frac{X}{\sqrt{1+X^2}} \right]^{\frac{1}{2}}, \quad (\text{A.6})$$

with a dimensionless parameter,

$$X = \frac{\mu_B B}{a} \left(g_e + \frac{m_e}{m_\mu} g_\mu \right) \simeq 6.31 \frac{B}{\text{Tesla}}, \quad (\text{A.7})$$

where $\mu_B = e/(2m_e)$ is the Bohr magneton, $g_e \simeq g_\mu \simeq 2$ is the magnetic moment of the electron/muon, and $a \simeq 1.846 \times 10^{-5} \text{ eV}$ is the $1S$ muonium hyperfine splitting. Similarly, the antimuonium states are represented as

$$|\bar{M}; 0, 0\rangle_B = \frac{c+s}{\sqrt{2}} |\bar{M}; 0, 0\rangle_0 - \frac{c-s}{\sqrt{2}} |\bar{M}; 1, 0\rangle_0, \quad (\text{A.8})$$

$$|\bar{M}; 1, 0\rangle_B = \frac{c+s}{\sqrt{2}} |\bar{M}; 1, 0\rangle_0 + \frac{c-s}{\sqrt{2}} |\bar{M}; 0, 0\rangle_0. \quad (\text{A.9})$$

The transition probability of $M \rightarrow \bar{M}$ under the nonzero B field is denoted as

$$P_{M\bar{M}} \simeq |c_{0,0}|^2 P_{M\bar{M}}^{(0,0)} + |c_{1,0}|^2 P_{M\bar{M}}^{(1,0)}, \quad (\text{A.10})$$

where $|c_{J,m_J}|$ is the population probability of the muonium initial state with (J, m_J) , which satisfies $|c_{0,0}|^2 + |c_{1,-1}|^2 + |c_{1,0}|^2 + |c_{1,1}|^2 = 1$. Note that the transitions of $|M; 0, 0\rangle_B \rightarrow |\bar{M}; 1, 0\rangle_B$ and $|M; 1, 0\rangle_B \rightarrow |\bar{M}; 0, 0\rangle_B$ are extremely suppressed due to the hyperfine splitting, and that of $|M; 1, \pm 1\rangle_B \rightarrow |\bar{M}; 1, \pm 1\rangle_B$ is also suppressed because the energy levels of the initial and final states are modified under the nonzero magnetic field.

The transition probabilities are represented by the transition amplitudes as [48, 49],

$$P_{\bar{M}M}^{(0,0)} \simeq \frac{2}{\lambda^2} |\langle \bar{M}; 0, 0 | \mathcal{H}_{\text{eff}} | M; 0, 0 \rangle_B|^2, \quad P_{\bar{M}M}^{(1,0)} \simeq \frac{2}{\lambda^2} |\langle \bar{M}; 1, 0 | \mathcal{H}_{\text{eff}} | M; 1, 0 \rangle_B|^2, \quad (\text{A.11})$$

where $\lambda = (\tau_\mu)^{-1} \simeq 3.00 \times 10^{-19} \text{ GeV}$ is the muon decay rate. Using Eqs. (A.4)–(A.9), the transition amplitudes are written as

$$\langle \bar{M}; 0, 0 | \mathcal{H}_{\text{eff}} | M; 0, 0 \rangle_B = \frac{1 + 2sc}{2} \langle \bar{M}; 0, 0 | \mathcal{H}_{\text{eff}} | M; 0, 0 \rangle_0 - \frac{1 - 2sc}{2} \langle \bar{M}; 1, 0 | \mathcal{H}_{\text{eff}} | M; 1, 0 \rangle_0, \quad (\text{A.12})$$

$$\langle \bar{M}; 1, 0 | \mathcal{H}_{\text{eff}} | M; 1, 0 \rangle_B = -\frac{1 - 2sc}{2} \langle \bar{M}; 0, 0 | \mathcal{H}_{\text{eff}} | M; 0, 0 \rangle_0 + \frac{1 + 2sc}{2} \langle \bar{M}; 1, 0 | \mathcal{H}_{\text{eff}} | M; 1, 0 \rangle_0. \quad (\text{A.13})$$

In the case of the effective Lagrangian of Eq. (2.5), when the ALP is sufficiently heavier than the muonium, the effective Hamiltonian is obtained by integrating the ALP field as

$$\mathcal{H}_{\text{eff}} = -\frac{(y_V)_{e\mu}^2}{m_a^2} S^2 - \frac{(y_A)_{e\mu}^2}{m_a^2} P^2, \quad (\text{A.14})$$

where $S = \bar{\mu}e$ and $P = \bar{\mu}\gamma_5 e$. Here, the CP conservation is assumed. Neglecting effects of the magnetic field, the transition matrix elements are [51]

$$\langle \bar{M}; F = 0 | S^2 | M; F = 0 \rangle_0 = \frac{2}{\pi a_B^3}, \quad \langle \bar{M}; F = 1 | S^2 | M; F = 1 \rangle_0 = -\frac{2}{\pi a_B^3}, \quad (\text{A.15})$$

$$\langle \bar{M}; F = 0 | P^2 | M; F = 0 \rangle_0 = -\frac{4}{\pi a_B^3}, \quad \langle \bar{M}; F = 1 | P^2 | M; F = 1 \rangle_0 = 0, \quad (\text{A.16})$$

where $a_B = 1/(m_r \alpha) \simeq 2.69 \times 10^5 (\text{GeV})^{-1}$ is the Bohr radius, and $m_r = m_e m_\mu / (m_e + m_\mu)$ is the reduced mass. Thus, we obtain

$$\langle \bar{M}; 0, 0 | \mathcal{H}_{\text{eff}} | M; 0, 0 \rangle_0 = -\frac{(y_V)_{e\mu}^2}{m_a^2} \frac{2}{\pi a_B^3} + \frac{(y_A)_{e\mu}^2}{m_a^2} \frac{4}{\pi a_B^3}, \quad (\text{A.17})$$

$$\langle \bar{M}; 1, 0 | \mathcal{H}_{\text{eff}} | M; 1, 0 \rangle_0 = \frac{(y_V)_{e\mu}^2}{m_a^2} \frac{2}{\pi a_B^3}. \quad (\text{A.18})$$

Consequently, the transition probabilities is derived as

$$P_{\text{MM}}^{(0,0)} = \frac{8}{\pi^2 a_B^6 \lambda^2} \left| \frac{(y_V)_{e\mu}^2}{m_a^2} - \left(1 + \frac{1}{\sqrt{1+X^2}}\right) \frac{(y_A)_{e\mu}^2}{m_a^2} \right|^2, \quad (\text{A.19})$$

$$P_{\text{MM}}^{(1,0)} = \frac{8}{\pi^2 a_B^6 \lambda^2} \left| \frac{(y_V)_{e\mu}^2}{m_a^2} - \left(1 - \frac{1}{\sqrt{1+X^2}}\right) \frac{(y_A)_{e\mu}^2}{m_a^2} \right|^2. \quad (\text{A.20})$$

Substituting them into Eq. (A.10), one obtains Eq. (4.1).

B Forward-backward asymmetry

In this appendix, the ALP contribution to the FB asymmetry of $e^+e^- \rightarrow \mu^+\mu^-$ is calculated. The asymmetry is obtained by an interference of the SM and ALP scattering amplitudes. In the former, a contribution with the virtual γ exchange dominates the amplitude for the energy $s \ll m_Z^2$. Then, it becomes

$$\mathcal{M}_\gamma = \frac{e^2}{s} (\bar{v}_{e^+} \gamma^\mu u_{e^-}) (\bar{u}_{\mu^-} \gamma_\mu v_{\mu^+}). \quad (\text{B.1})$$

We define θ^* as the angle between μ^+ and e^+ in the center-of-mass frame. The integration of the squared amplitude over $\cos \theta^*$ including a factor of the polarization sums leads to

$$\int_{-1}^1 d(\cos \theta^*) \left(\frac{1}{2}\right)^2 |\mathcal{M}_\gamma|^2 = \frac{8}{3} e^4 \left(1 + \frac{2m_\mu^2}{s}\right), \quad (\text{B.2})$$

which gives a normalization for A_{FB} . Note that $|\mathcal{M}_\gamma|^2$ does not generate A_{FB} . On the other hand, the ALP amplitude is obtained as

$$\begin{aligned} \mathcal{M}_a = & \frac{1}{2(k^2 - m_a^2)} \left\{ \left| (y_V)_{e\mu} - (y_A)_{e\mu} \right|^2 (\bar{v}_{e^+} \gamma^\mu P_R u_{e^-}) (\bar{u}_{\mu^-} \gamma_\mu P_L v_{\mu^+}) \right. \\ & \left. + \left| (y_V)_{e\mu} + (y_A)_{e\mu} \right|^2 (\bar{v}_{e^+} \gamma^\mu P_L u_{e^-}) (\bar{u}_{\mu^-} \gamma_\mu P_R v_{\mu^+}) \right\} \\ & + \frac{1}{2(k^2 - m_a^2)} \left\{ \left[\left| (y_V)_{e\mu} \right|^2 - \left| (y_A)_{e\mu} \right|^2 + 2i \text{Im} (y_V)_{e\mu} (y_V)_{e\mu}^* \right] \right. \\ & \times \left[(\bar{v}_{e^+} P_L u_{e^-}) (\bar{u}_{\mu^-} P_L v_{\mu^+}) + \frac{1}{4} (\bar{v}_{e^+} \sigma^{\mu\nu} P_L u_{e^-}) (\bar{u}_{\mu^-} \sigma_{\mu\nu} P_L v_{\mu^+}) \right] \\ & + \left[\left| (y_V)_{e\mu} \right|^2 - \left| (y_A)_{e\mu} \right|^2 - 2i \text{Im} (y_V)_{e\mu} (y_V)_{e\mu}^* \right] \\ & \left. \times \left[(\bar{v}_{e^+} P_R u_{e^-}) (\bar{u}_{\mu^-} P_R v_{\mu^+}) + \frac{1}{4} (\bar{v}_{e^+} \sigma^{\mu\nu} P_R u_{e^-}) (\bar{u}_{\mu^-} \sigma_{\mu\nu} P_R v_{\mu^+}) \right] \right\}, \quad (\text{B.3}) \end{aligned}$$

after the Fierz rearrangement of the fermion order. Here, $\sigma^{\mu\nu} = \frac{i}{2}[\gamma^\mu, \gamma^\nu]$ and

$$k^2 = m_\mu^2 - \frac{s}{2} + \sqrt{s \left(\frac{s}{4} - m_\mu^2 \right)} \cos \theta^*. \quad (\text{B.4})$$

Discarding the electron mass, we obtain the interference term of γ and a as

$$\mathcal{I} = \left(\frac{1}{2} \right)^2 2\text{Re}(\mathcal{M}_\gamma \mathcal{M}_a^*) \quad (\text{B.5})$$

$$= \frac{e^2}{2(k^2 - m_a^2)} \left[\left| (y_V)_{e\mu} \right|^2 + \left| (y_A)_{e\mu} \right|^2 \right] \\ \times \left[s(1 + \cos^2 \theta^*) + 4m_\mu^2(1 - \cos^2 \theta^*) - 4\sqrt{s \left(\frac{s}{4} - m_\mu^2 \right)} \cos \theta^* \right]. \quad (\text{B.6})$$

Substituting this into a numerator in Eq. (5.4) with the denominator from Eq. (B.2), the ALP contribution to the FB asymmetry is derived as

$$A_{\text{FB}}^{\text{ALP}} \simeq \frac{3}{8e^4} \left(\int_0^1 d(\cos \theta^*) \mathcal{I} - \int_{-1}^0 d(\cos \theta^*) \mathcal{I} \right). \quad (\text{B.7})$$

for $s \gg m_\mu^2$. Note that the differential cross section is given as

$$\left(\frac{1}{2} \right)^2 |\mathcal{M}(e^+e^- \rightarrow \mu^+\mu^-)|^2 = 2e^4 \frac{s^2 + 2sk^2 + 2k^4 - 4m_\mu^2 k^2 + 2m_\mu^4}{s^2} \\ + 2e^2 \left[\left| (y_V)_{e\mu} \right|^2 + \left| (y_A)_{e\mu} \right|^2 \right] \frac{k^4 + m_\mu^2(s - 2k^2) + m_\mu^4}{s(k^2 - m_a^2)} \\ + \left[\left| (y_V)_{e\mu} \right|^2 + \left| (y_A)_{e\mu} \right|^2 \right]^2 \left(\frac{k^2 - m_\mu^2}{k^2 - m_a^2} \right)^2, \quad (\text{B.8})$$

where the second line corresponds to the interference term.

References

- [1] **Muon g-2** Collaboration, *Measurement of the positive muon anomalous magnetic moment to 0.7 ppm*, *Phys. Rev. Lett.* **89** (2002) 101804 [[hep-ex/0208001](#)]. [Erratum: *Phys. Rev. Lett.* **89** (2002) 129903].
- [2] **Muon g-2** Collaboration, *Measurement of the negative muon anomalous magnetic moment to 0.7 ppm*, *Phys. Rev. Lett.* **92** (2004) 161802 [[hep-ex/0401008](#)].
- [3] **Muon g-2** Collaboration, *Final Report of the Muon E821 Anomalous Magnetic Moment Measurement at BNL*, *Phys. Rev.* **D73** (2006) 072003 [[hep-ex/0602035](#)].

- [4] M. Endo, K. Hamaguchi, S. Iwamoto, and T. Kitahara, *Muon $g - 2$ vs LHC Run 2 in Supersymmetric Models*. [arXiv:2001.11025](#).
- [5] T. Aoyama, M. Hayakawa, T. Kinoshita, and M. Nio, *Complete Tenth-Order QED Contribution to the Muon $g - 2$* , *Phys. Rev. Lett.* **109** (2012) 111808 [[arXiv:1205.5370](#)].
- [6] T. Aoyama, T. Kinoshita, and M. Nio, *Revised and Improved Value of the QED Tenth-Order Electron Anomalous Magnetic Moment*, *Phys. Rev.* **D97** (2018) 036001 [[arXiv:1712.06060](#)].
- [7] S. Volkov, *Calculating the five-loop QED contribution to the electron anomalous magnetic moment: Graphs without lepton loops*, *Phys. Rev.* **D100** (2019) 096004 [[arXiv:1909.08015](#)].
- [8] M. Knecht, S. Peris, M. Perrottet, and E. De Rafael, *Electroweak hadronic contributions to the muon ($g-2$)*, *JHEP* **11** (2002) 003 [[hep-ph/0205102](#)].
- [9] A. Czarnecki, W. J. Marciano, and A. Vainshtein, *Refinements in electroweak contributions to the muon anomalous magnetic moment*, *Phys. Rev.* **D67** (2003) 073006 [[hep-ph/0212229](#)]. [Erratum: *Phys. Rev.* **D73** (2006) 119901].
- [10] C. Gnendiger, D. Stöckinger, and H. Stöckinger-Kim, *The electroweak contributions to $(g - 2)_\mu$ after the Higgs boson mass measurement*, *Phys. Rev.* **D88** (2013) 053005 [[arXiv:1306.5546](#)].
- [11] T. Ishikawa, N. Nakazawa, and Y. Yasui, *Numerical calculation of the full two-loop electroweak corrections to muon ($g-2$)*, *Phys. Rev.* **D99** (2019) 073004 [[arXiv:1810.13445](#)].
- [12] M. Davier, A. Hoecker, B. Malaescu, and Z. Zhang, *A new evaluation of the hadronic vacuum polarisation contributions to the muon anomalous magnetic moment and to $\alpha(m_Z^2)$* . [arXiv:1908.00921](#).
- [13] A. Keshavarzi, D. Nomura, and T. Teubner, *The $g - 2$ of charged leptons, $\alpha(M_Z^2)$ and the hyperfine splitting of muonium*, *Phys. Rev.* **D101** (2020) 014029 [[arXiv:1911.00367](#)].
- [14] J. Prades, E. de Rafael, and A. Vainshtein, *The Hadronic Light-By-Light Scattering Contribution to the Muon and Electron Anomalous Magnetic Moments*, *Adv. Ser. Direct. High Energy Phys.* **20** (2009) 303–317 [[arXiv:0901.0306](#)].
- [15] T. Blum, *et al.*, *The hadronic light-by-light scattering contribution to the muon anomalous magnetic moment from lattice QCD*. [arXiv:1911.08123](#).
- [16] **Muon $g-2$ Collaboration**, *Muon $g - 2$ Technical Design Report*. [arXiv:1501.06858](#).

- [17] **Muon g-2** Collaboration, *The Muon $g - 2$ Experiment at Fermilab*, *EPJ Web Conf.* **212** (2019) 05003 [[arXiv:1905.00497](#)].
- [18] **J-PARC g-2** Collaboration, *Measurement of muon $g - 2$ and EDM with an ultra-cold muon beam at J-PARC*, *Nucl. Phys. Proc. Suppl.* **218** (2011) 242–246.
- [19] M. Abe *et al.*, *A New Approach for Measuring the Muon Anomalous Magnetic Moment and Electric Dipole Moment*, *PTEP* **2019** (2019) 053C02 [[arXiv:1901.03047](#)].
- [20] R. H. Parker, C. Yu, W. Zhong, B. Estey, and H. Müller, *Measurement of the fine-structure constant as a test of the Standard Model*, *Science* **360** (2018) 191 [[arXiv:1812.04130](#)].
- [21] R. Bouchendir, P. Clade, S. Guellati-Khelifa, F. Nez, and F. Biraben, *New determination of the fine structure constant and test of the quantum electrodynamics*, *Phys. Rev. Lett.* **106** (2011) 080801 [[arXiv:1012.3627](#)].
- [22] D. Hanneke, S. Fogwell, and G. Gabrielse, *New Measurement of the Electron Magnetic Moment and the Fine Structure Constant*, *Phys. Rev. Lett.* **100** (2008) 120801 [[arXiv:0801.1134](#)].
- [23] A. Crivellin, M. Hoferichter, and P. Schmidt-Wellenburg, *Combined explanations of $(g - 2)_{\mu,e}$ and implications for a large muon EDM*, *Phys. Rev.* **D98** (2018) 113002 [[arXiv:1807.11484](#)].
- [24] J. Liu, C. E. M. Wagner, and X.-P. Wang, *A light complex scalar for the electron and muon anomalous magnetic moments*, *JHEP* **03** (2019) 008 [[arXiv:1810.11028](#)].
- [25] M. Endo and W. Yin, *Explaining electron and muon $g - 2$ anomaly in SUSY without lepton-flavor mixings*, *JHEP* **08** (2019) 122 [[arXiv:1906.08768](#)].
- [26] M. Badziak and K. Sakurai, *Explanation of electron and muon $g - 2$ anomalies in the MSSM*, *JHEP* **10** (2019) 024 [[arXiv:1908.03607](#)].
- [27] A. E. Cárcamo Hernández, S. F. King, H. Lee, and S. J. Rowley, *Is it possible to explain the muon and electron $g - 2$ in a Z' model?* [arXiv:1910.10734](#).
- [28] H. Davoudiasl and W. J. Marciano, *Tale of two anomalies*, *Phys. Rev.* **D98** (2018) 075011 [[arXiv:1806.10252](#)].
- [29] X.-F. Han, T. Li, L. Wang, and Y. Zhang, *Simple interpretations of lepton anomalies in the lepton-specific inert two-Higgs-doublet model*, *Phys. Rev.* **D99** (2019) 095034 [[arXiv:1812.02449](#)].
- [30] B. Dutta and Y. Mimura, *Electron $g - 2$ with flavor violation in MSSM*, *Phys. Lett.* **B790** (2019) 563–567 [[arXiv:1811.10209](#)].

- [31] M. Bauer, M. Neubert, S. Renner, M. Schnubel, and A. Thamm, *Axion-like particles, lepton-flavor violation and a new explanation of a_μ and a_e* . [arXiv:1908.00008](#).
- [32] C. Cornella, P. Paradisi, and O. Sumensari, *Hunting for ALPs with Lepton Flavor Violation*, [JHEP **01** \(2020\) 158](#) [[arXiv:1911.06279](#)].
- [33] D. B. Reiss, *Can the Family Group Be a Global Symmetry?* [Phys. Lett. **115B** \(1982\) 217–220](#).
- [34] G. B. Gelmini, S. Nussinov, and T. Yanagida, *Does Nature Like Nambu-Goldstone Bosons?* [Nucl. Phys. **B219** \(1983\) 31–40](#).
- [35] F. Wilczek, *Axions and Family Symmetry Breaking*, [Phys. Rev. Lett. **49** \(1982\) 1549–1552](#).
- [36] A. A. Anselm, N. G. Uraltsev, and M. Yu. Khlopov, *$\mu \rightarrow e$ FAMILON DECAY*, [Sov. J. Nucl. Phys. **41** \(1985\) 1060](#). [[Yad. Fiz.41,1678\(1985\)](#)].
- [37] J. L. Feng, T. Moroi, H. Murayama, and E. Schnapka, *Third generation familons, b factories, and neutrino cosmology*, [Phys. Rev. **D57** \(1998\) 5875–5892](#) [[hep-ph/9709411](#)].
- [38] J. Martin Camalich, M. Pospelov, P. N. H. Vuong, R. Ziegler, and J. Zupan, *Quark Flavor Phenomenology of the QCD Axion*. [arXiv:2002.04623](#).
- [39] H. Georgi, D. B. Kaplan, and L. Randall, *Manifesting the Invisible Axion at Low-energies*, [Phys. Lett. **169B** \(1986\) 73–78](#).
- [40] M. Bauer, M. Neubert, and A. Thamm, *Collider Probes of Axion-Like Particles*, [JHEP **12** \(2017\) 044](#) [[arXiv:1708.00443](#)].
- [41] P. S. B. Dev, R. N. Mohapatra, and Y. Zhang, *Lepton Flavor Violation Induced by a Neutral Scalar at Future Lepton Colliders*, [Phys. Rev. Lett. **120** \(2018\) 221804](#) [[arXiv:1711.08430](#)].
- [42] Y. Abe, T. Toma, and K. Tsumura, *A μ - τ -philic scalar doublet under Z_n flavor symmetry*, [JHEP **06** \(2019\) 142](#) [[arXiv:1904.10908](#)].
- [43] S. Nie and M. Sher, *The Anomalous magnetic moment of the muon and Higgs mediated flavor changing neutral currents*, [Phys. Rev. **D58** \(1998\) 097701](#) [[hep-ph/9805376](#)].
- [44] I. Galon, A. Kwa, and P. Tanedo, *Lepton-Flavor Violating Mediators*, [JHEP **03** \(2017\) 064](#) [[arXiv:1610.08060](#)].
- [45] **TWIST** Collaboration, *Search for two body muon decay signals*, [Phys. Rev. **D91** \(2015\) 052020](#) [[arXiv:1409.0638](#)].

- [46] **ACME** Collaboration, *Improved limit on the electric dipole moment of the electron*, *Nature* **562** (2018) 355–360.
- [47] B. Pontecorvo, *Mesonium and anti-mesonium*, *Sov. Phys. JETP* **6** (1957) 429. [*Zh. Eksp. Teor. Fiz.*33,549(1957)].
- [48] G. Feinberg and S. Weinberg, *Law of Conservation of Muons*, *Phys. Rev. Lett.* **6** (1961) 381–383.
- [49] G. Feinberg and S. Weinberg, *Conversion of Muonium into Antimuonium*, *Phys. Rev.* **123** (1961) 1439–1443.
- [50] M. L. Swartz, *Limits on Doubly Charged Higgs Bosons and Lepton Flavor Violation*, *Phys. Rev.* **D40** (1989) 1521.
- [51] W.-S. Hou and G.-G. Wong, $\mu^+e^- \leftrightarrow \mu^-e^+$ transitions via neutral scalar bosons, *Phys. Rev.* **D53** (1996) 1537–1541 [[hep-ph/9504311](#)].
- [52] W.-S. Hou and G.-G. Wong, *Magnetic field dependence of muonium - anti-muonium conversion*, *Phys. Lett.* **B357** (1995) 145–150 [[hep-ph/9505300](#)].
- [53] K. Horikawa and K. Sasaki, *Muonium - anti-muonium conversion in models with dilepton gauge bosons*, *Phys. Rev.* **D53** (1996) 560–563 [[hep-ph/9504218](#)].
- [54] S. L. Glashow, *Direct Xi Decay and Muonium-Antimuonium Transitions*, *Phys. Rev. Lett.* **6** (1961) 196–197.
- [55] L. Willmann *et al.*, *New bounds from searching for muonium to anti-muonium conversion*, *Phys. Rev. Lett.* **82** (1999) 49–52 [[hep-ex/9807011](#)].
- [56] R. Harnik, J. Kopp, and J. Zupan, *Flavor Violating Higgs Decays*, *JHEP* **03** (2013) 026 [[arXiv:1209.1397](#)].
- [57] J. E. Kim, P. Ko, and D.-G. Lee, *More on R-parity and lepton family number violating couplings from muon(ium) conversion, and τ and π^0 decays*, *Phys. Rev.* **D56** (1997) 100–106 [[hep-ph/9701381](#)].
- [58] J. A. Evans, P. Tanedo, and M. Zakeri, *Exotic Lepton-Flavor Violating Higgs Decays*, *JHEP* **01** (2020) 028 [[arXiv:1910.07533](#)].
- [59] K. Hanagaki, H. Kakuno, H. Ikeda, T. Iijima, and T. Tsukamoto, *Electron identification in Belle*, *Nucl. Instrum. Meth.* **A485** (2002) 490–503 [[hep-ex/0108044](#)].
- [60] **Belle** Collaboration, *Evidence of the Purely Leptonic Decay $B^- \rightarrow \tau^- \bar{\nu}_\tau$* , *Phys. Rev. Lett.* **97** (2006) 251802 [[hep-ex/0604018](#)].

- [61] **Belle-II** Collaboration, *The Belle II Physics Book*, **PTEP** **2019** (2019) 123C01 [[arXiv:1808.10567](#)].
- [62] S. Iguro, Y. Omura, and M. Takeuchi, *Testing the 2HDM explanation of the muon $g - 2$ anomaly at the LHC*, **JHEP** **11** (2019) 130 [[arXiv:1907.09845](#)].
- [63] J. Alwall, *et al.*, *The automated computation of tree-level and next-to-leading order differential cross sections, and their matching to parton shower simulations*, **JHEP** **07** (2014) 079 [[arXiv:1405.0301](#)].
- [64] A. Alloul, N. D. Christensen, C. Degrande, C. Duhr, and B. Fuks, *FeynRules 2.0 - A complete toolbox for tree-level phenomenology*, **Comput. Phys. Commun.** **185** (2014) 2250–2300 [[arXiv:1310.1921](#)].
- [65] T. Ferber, *Towards First Physics at Belle II*, **Acta Phys. Polon.** **B46** (2015) 2285.
- [66] **Belle**, **Belle-II** Collaboration, *Perspectives of a precise measurement of the charge asymmetry in muon pair production at Belle II*, **J. Univ. Sci. Tech. China** **46** (2016) 476–480.
- [67] J. de Blas, *et al.*, *Electroweak precision observables and Higgs-boson signal strengths in the Standard Model and beyond: present and future*, **JHEP** **12** (2016) 135 [[arXiv:1608.01509](#)].
- [68] F. Jegerlehner, *Precision measurements of σ_{hadronic} for $\alpha_{\text{eff}}(E)$ at ILC energies and $(g - 2)_\mu$* , **Nucl. Phys. Proc. Suppl.** **162** (2006) 22–32 [[hep-ph/0608329](#)].
- [69] F. Jegerlehner in *Theory report on the 11th FCC-ee workshop*, pp. 9–37. 2019.
- [70] **ALEPH**, **DELPHI**, **L3**, **OPAL**, **LEP Electroweak** Collaboration, *Electroweak Measurements in Electron-Positron Collisions at W-Boson-Pair Energies at LEP*, **Phys. Rept.** **532** (2013) 119–244 [[arXiv:1302.3415](#)].